

Study of Reaction Between Slag and Carbonaceous Materials



SAMANE MAROUFI, MOHANNAD MAYYAS, IRSHAD MANSURI, PAUL O'KANE, CATHERINE SKIDMORE, ZHESHI JIN, ANDREA FONTANA, and VEENA SAHAJWALLA

The chemical interaction of a typical slag of EAF with three different carbon sources, coke, rubber-derived carbon (RDC), coke-RDC blend, was studied in atmospheric pressure at 1823 K (1550 °C). Using an IR-gas analyzer, off-gases evolved from the sample were monitored. While the coke-RDC blend exhibited the best reducing performance in reaction with molten slag, the RDC sample showed poor interaction with the molten slag. The gasification of the coke, RDC, and coke-RDC blend was also carried out under oxidizing conditions using a gas mixture of CO₂ (4 wt pct) and Ar (96 wt pct) and it was shown that the RDC sample had the highest rate of gasification step $C_0 \rightarrow k_3CO + nC_f$ (11.6 site/g s ($\times 6.023 \times 10^{23} / 2.24 \times 10^4$)). This may be attributed to its disordered structure confirmed by Raman spectra and its nano-particle morphology observed by FE-SEM. The high reactivity of RDC with CO₂ provided evidence that the Boudouard reaction was fast during the interaction with molten slag. However, low reduction rate of iron oxide from slag with RDC can be attributed to the initial weak contact between RDC and molten slag implying that the contact between carbonaceous matter and slag plays significant roles in the reduction of iron oxide from slag.

DOI: 10.1007/s11663-017-1020-y

© The Minerals, Metals & Materials Society and ASM International 2017

I. INTRODUCTION

IN electric arc furnace (EAF) steelmaking, slag foaming plays a key role in reducing the consumption and, therefore, the cost of energy, by improving the efficiency and stability of the furnace and by decreasing sound, vibration, and electrode consumption during the process of melting.^[1] Foamy slag in EAF steelmaking is formed by injecting carbon from different sources. In recent years, the utilization of waste tyre rubbers (WTR) in EAF steelmaking and its effect on slag foaming behavior have been widely investigated.^[2–8] Using *Polymer Injection Technology* (PIT), a meaningful proportion of metallurgical coke can be substituted by granulated end-of-life waste rubber, as a carbon injectant.^[9] In previous work,^[4,6] it has been shown that a

precisely calibrated mix of granulated waste rubber and coke improves the foaminess of slag.

In the slag foaming phenomenon, the molten slag expands due to the evolution of CO/CO₂ gas bubbles from the chemical reactions which take place at the slag-carbon interface. The slag-carbon interaction is a dynamic process, in respect to the chemical reactions that occur, as the composition of the slag is continually changing. The mechanism of the reactions between the solid carbon and iron oxide present in the slag occur *via* intermediate gases. CO gas produced in the initial stages of reactions between the carbon source and the slag is transported through the gas phase and reacts with the iron oxide in the slag to produce CO₂ and metallic iron. This CO₂ is then ferried back to carbon, and gasification of CO₂ to CO takes place *via* the Boudouard reaction. The kinetics of the reactions between iron oxide in the slag and the carbon source play an important role in the steelmaking process. Numerous studies have been carried out on the reduction of iron oxide in molten slag and the effect of the carbon injection on the rate of reduction.^[10–13]

In a work published by Ozawa *et al.*,^[10] the effect of the injection of solid carbon on the reduction rate of FeO in slag in EAF steelmaking was discussed in relation to the quality and size of the carbon powder injected, the injection rate, and nature of the molten slag. They found that the type and quality of the solid

SAMANE MAROUFI, MOHANNAD MAYYAS, IRSHAD MANSURI, and VEENA SAHAJWALLA are with the Centre for Sustainable Materials Research and Technology (SMaRT), School of Materials Science and Engineering, University of New South Wales, Sydney, NSW, 2052, Australia. Contact e-mail: s.maroufi@unsw.edu.au PAUL O'KANE, CATHERINE SKIDMORE, and ZHESHI JIN are with OneSteel, Rooty Hill, Sydney, NSW, 2766, Australia. ANDREA FONTANA is with OneSteel, Laverton, Melbourne, VIC, 3026, Australia.

Manuscript submitted March 7, 2017.

Article published online June 23, 2017.

carbon injected and, in particular, the presence of volatile matter in the solid carbon affect reduction. According to their work, three major factors (the quality of the solid carbon, the boundary area of reaction wherein solid carbon reacts with FeO, and the nature of the slag) control the reduction rate of FeO in slag.

Later, in 1995, Lee and Lee^[11] published the results of their research on the reduction behavior of FeO in EAF slag. In their paper, they discussed the effect of residence refining time (*i.e.*, from meltdown-to-tap) on the recovery of metal value from the molten slag. They found an increase in residence refining time which resulted in the complete reduction of iron oxide to metallic iron.

Ji *et al.*^[12] carried out a kinetic study of carbon injection in EAF steelmaking. They measured the rate of carbon oxidation during injection at temperatures from 1866 K to 1975 K (1593 °C to 1702 °C) using coal as the injectant. They estimated the rate of reaction of low volatile coal with EAF slag at a moderate injection rate of coal and found that at lower injection rate, the gasification rate strongly depended upon the injection rate of coal.

The utilization of WTR as carbon injectant has been extensively investigated in relation to its effect on the slag foaming phenomenon. In the previous work,^[13] it has been shown that by mixing coke and WTR in a particular ratio, slag foaming could be significantly improved. However, the effect of the partial substitution of coke by rubber-derived carbon (RDC) on the reduction of iron oxide from molten slag during the phenomenon of slag foaming has not been reported previously. This work aims to study the reduction of iron oxide from industrial slag using metallurgical coke, RDC, and coke-RDC blend and investigate its effect on the rate of reduction.

II. MATERIALS AND EXPERIMENTAL PROCEDURE

The ultimate, proximate, and elemental analyses of WTR and coke and chemical compositions of slag are displayed in Tables I and II.

The WTR was treated in a high-temperature tubular furnace at 1823 K (1550 °C) for 5 seconds under argon purge (1 L min⁻¹); the resulting black char was subsequently ground using a ring mill followed by 30 minutes of mixing in a roll mill for better homogeneity, and thus rubber-derived carbon (RDC) was prepared. In the case of the coke-RDC blend, metallurgical coke and RDC were mixed in a particular proportion (based on our previous study of the best proportion for slag foaming^[4,6]) and the blends were then crushed using a jaw crusher to increase the uniformity in particle size distribution. After crushing, samples were sieved into different particle sizes and particles in the range from 106 to 200 μm were selected for this study. Hydraulic press was utilized to press the powder samples with a pressure of 150 MPa without a binder (diameter of 20 mm and a thickness of 3 to 4 mm). Interactions between carbons and slag at elevated temperatures were

studied by placing about 0.07 g of slag on the top of the disk-shaped pellets.

Slag and disk-shaped pellets were placed on an alumina crucible and carefully inserted into a preheated tubular furnace using a graphite rod. After specific reaction time, the sample was withdrawn from the hot zone of the furnace to the cold zone, and then left to cool down to room temperature under argon atmosphere.

The furnace was connected to an infrared gas analyzer (ABB, Advance Optima Series AO2020) in order to monitor off-gases evolved from the system during the process of reduction. After completing the experiments described above, samples were collected and characterized using different analytical techniques. An X'pert PRO Multi-purpose XRD (MPD system), operating at 40 kV and 40 mA with measurement recording in the range of $2\theta = 0$ to 100 deg was used to analyze the crystalline component of the sample. Raman spectra were obtained using Renishaw inVia Raman Microscope to determine the molecular structure of the carbonaceous materials. FEI Nova-SEM 230 (FE-SEM) configured with a Bruker SDD-EDS detector was used to study the physical structure and morphology of the samples. Prior to analysis, a coating of platinum was applied to samples using a Cressington 208 HR Sputter Coater.

III. RESULTS AND DISCUSSION

A. Heat Treatment of the Samples in Argon

Coke, RDC, and coke-RDC blend pellets were heated at 1823 K (1550 °C) in 1 atm pressure under argon purge (1 L min⁻¹). An IR-gas analyzer was utilized to monitor CO, CO₂, and CH₄ gases evolved from the samples. Figure 1 illustrates the CO, CO₂, and CH₄ concentration (ppm) as a function of reaction time. In all cases, in the first 50 seconds, the concentration of CO gas surged, indicating sample decomposition. In Figure 1(a), after 200 seconds, a slight increase in CO concentration is observed which can be attributed to the carbothermal reduction of oxide mineral content (*i.e.*, ash) such as SiO₂. According to the ultimate analysis (Table I), metallurgical coke contains about 11 wt pct mineral ash. During the process of heat treatment, SiO₂ of the mineral ash reacted with carbon and SiC was formed. In coke-RDC blend (Figure 1(c)), the same increase trend in CO concentration was observed. In comparison to the concentration of CO in the off-gases, the concentrations of CO₂ and CH₄ were negligible.

B. Heat Treatment of the Samples in Argon with the Addition of Slag

Under the same conditions, experiments were carried out while 0.07 g of industrial EAF slag was placed on the top of the pellets. The concentrations of CO, CO₂, and CH₄ gases evolved from the system were also monitored using an IR-gas analyzer. Figure 1 shows the concentration of gases generated during the experiment

Table I. Coke and WTR Analysis

	Carbon		Hydrogen		Nitrogen		Sulfur		Oxygen		
Ultimate Analysis (Weight Pct)											
WTR	83.8		7.13		0.37		2		6.7		
Coke	86.6		0.49		1.32		0.48		0		
	Volatile Matter			Fixed Carbon			Moisture		Ash		
Proximate Analysis (Weight Pct)											
WTR	63.2			30.2			0.9		5.7		
Coke	15			55.5			4		11		
	SiO ₂	Fe ₂ O ₃	Al ₂ O ₃	CaO	MgO	Na ₂ O	K ₂ O	P ₂ O ₅	SO ₃	TiO ₂	ZnO
Chemical Composition of Mineral Ash (Weight Pct)											
WTR	27.9	0.14	3.1	8.4	1.3	1.4	0.05	—	7.58	—	40.8
Coke	50.7	4.8	36.0	3.3	0.9	0.4	0.5	1.6	0.4	1.4	—

Table II. The Slag Chemical Composition (Weight Percent)

Fe ₂ O ₃	SiO ₂	Al ₂ O ₃	CaO	MgO	MnO
36.2	12.4	6.4	29.2	11.3	5.7

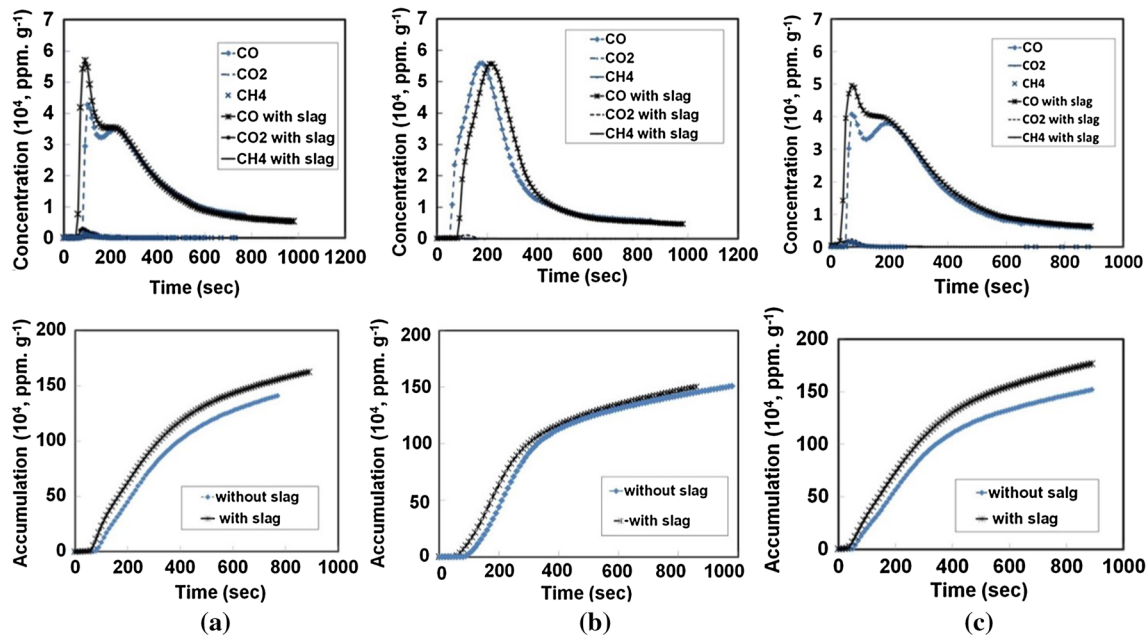


Fig. 1—Generated gas concentration in terms of CO, CO₂, and CH₄ gases and the accumulation of generated gases (CO + CO₂ + CH₄) evolved due to the heat treatment of (a) coke, (b) RDC, and (c) coke-RDC blend with and without slag in argon at 1823 K (1550 °C).

with slag. By placing slag on the top of the pellets, the reduction of iron oxide by carbonaceous materials (coke, RDC, and coke-RDC blend) was expected to occur, therefore resulting in higher concentrations of CO–CO₂ in the off-gases. In the cases of the coke and coke-RDC blend samples, the increase in the concentration of CO in the off-gases can be clearly observed, implying that iron oxide reduction by carbon sources occurred. However, the concentration of CO evolved from the interaction between RDC pellet and industrial

slag was found to be equivalent to the concentration of CO from RDC pellet alone. The accumulation and concentration of gases evolved over time are illustrated in Figure 1. While the coke-RDC sample exhibited the largest difference in terms of the concentration of CO + CO₂ + CH₄ in the off-gases for experiments with and without slag, pure RDC showed only a slight difference.

Coke, RDC, and coke-RDC blend pellets after heat treatment prior to the addition of slag were investigated

by XRD technique. Figure 2, presents the XRD pattern of coke, RDC, and coke-RDC blend pellets after heat treatment in argon. In all spectra's, SiC and carbon peaks were observed over the examined range (10 to 80 deg). Strong SiC peaks were observed in the case of coke and coke-RDC, that can be attributed to a high content of mineral ash in the coke.

As can be observed in Figure 2, each diffraction pattern displays a broad diffraction peak at around 25 deg, which corresponds to the diffraction from 002 crystal plane of graphitic carbon. According to the XRD analysis and using Bragg's law Eq. [1], the interlayer spacing (d_{002}) of each sample was calculated and listed in Table III. The coke and coke-RDC blend show the smallest spacing with approximately 3.41 Å, which is close to ideal crystalline graphite (3.4 Å). The RDC sample shows a slightly higher value of approximately 3.5 Å. The crystallite size (L_c) is another important factor that determines the crystallinity of the graphitic structure. The L_c value of each sample was calculated using Scherrer's formula (Eq. [2]). As shown in Table III, RDC has a relatively large L_c value of around 4.7 nm, while coke and the coke-RDC blend had smaller values of 3 and 2.2 nm, respectively. The smaller d-spacing values could imply an ideal graphitic structure with lesser defects. The coke-RDC and coke samples show a relatively small d-spacing with a small L_c , and they could therefore be expected to have an ideal structure with high crystallinity.

$$d_{hkl} = \frac{0.1542}{2\sin\left(\theta \text{ deg} \cdot \frac{\pi}{180\text{deg}}\right)} \quad [1]$$

$$L_c = \frac{0.1449}{\text{FWHM deg}} \cdot \frac{\pi}{180\text{deg}} \cdot \cos(\theta \text{ deg}). \quad [2]$$

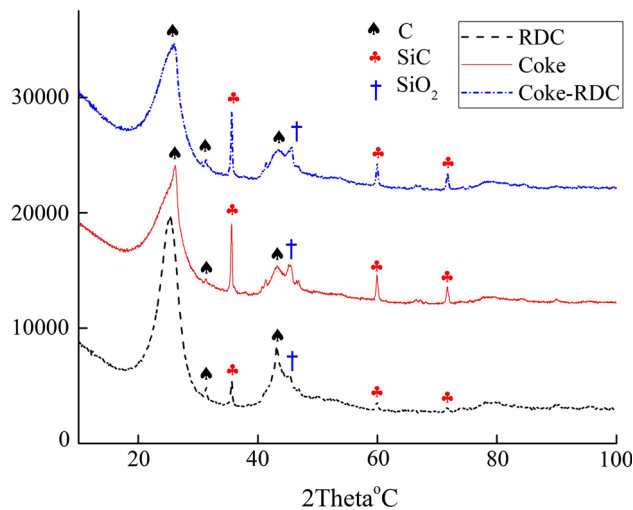
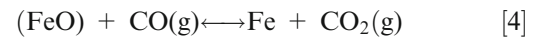


Fig. 2—XRD spectra of coke, RDC, and coke-RDC blend after heat treatment in argon at 1823 K (1550 °C) prior to the addition of slag.

C. Reactivity Measurement in CO_2

In the slag-carbonaceous material reaction, the reduction of iron oxide occurs through intermediate CO/CO_2 gases. The mechanism of carbothermal reduction of iron oxide from slags has been widely reported in the literature.^[13–17]

The initial contact between the carbon substrate and the slag leads to the reduction of FeO from slag by solid carbon and the formation of CO gas (Reaction [3]). The produced CO reacts with FeO resulting in generation of CO_2 (Reaction [4]) which in turn reacts with carbon (Reaction [5]). During this carbothermal reduction process, the Boudouard reaction plays a key role, as the CO generated from this reaction is a reducing agent for the reduction of oxide.

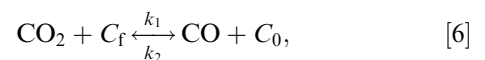


It is worth noting that the whole process involves gas–liquid, gas–solid, and even solid–liquid reactions, as well as mass transfer in the gas and slag phases. To understand these phenomena, a number of authors have studied the reduction behavior of iron oxides thermodynamically and kinetically.

The Boudouard reaction occurs simultaneously with iron oxide reduction in all reactions, acting as a driving force for chemical reactions. It is known that the complimentary Boudouard reaction is the controlling reaction in the process of carbothermal reduction of iron oxide. The rate of Boudouard reaction can play a key role in the process of reduction.

Gasification experiments with the prepared coke, RDC, and coke-RDC pellets were conducted in CO_2 to compare the reactivity of carbonaceous matters. Experiments were carried out at 1823 K (1550 °C) in $Ar(96 \text{ pct})-CO_2(4 \text{ pct})$ mixture (1 L min^{-1}). The same mass of carbonaceous materials (1 g) was used in all experiments. The off-gases evolved from the furnace due to gasification reactions were analyzed using an Ar -gas analyzer. Figure 3, represents the concentration of CO and CO_2 in the off-gases released from the coke, RDC, and coke-RDC blend samples during gasification in CO_2 .

Numerous researchers have demonstrated^[18–23] that in the reaction between carbonaceous material and CO_2 , certain carbon atoms, known as reaction sites, can detach an oxygen atom from a carbon dioxide molecule. Conversely, the oxygen retained on the surface can react with CO according to the following reaction:



where C_f is a free site capable of detaching an oxygen atom from CO_2 , C_0 representative of an occupied site which possess an oxygen atom. k_1 and k_2 are reaction rate constants which are functions of temperature

Table III. Crystallographic Data of Graphite Structure in Coke, RDC, and Coke-RDC Blend

	2θ	d -Spacing (\AA)	FWHM	Crystallite Size (L_c , nm)
RDC	25.4	3.5	3.0	4.7
Coke	26.1	3.4	5.1	3.0
Coke-RDC blend	25.8	3.41	4.7	2.2

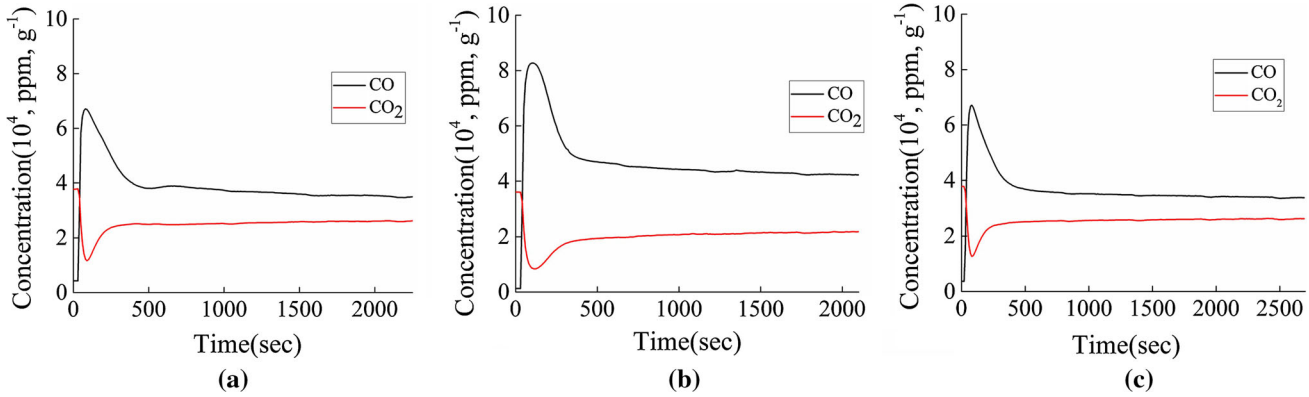
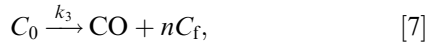


Fig. 3—Generated gas concentration in terms of CO and CO₂ gases evolved due to the heat treatment of (a) coke, (b) RDC, and (c) coke-RDC blend in CO₂-Ar mixture at 1823 K (1550 °C).

only. This reaction is known as an oxygen-exchange reaction.

A carbon atom from the occupied site in solid phase can be transferred to the gas phase:



where k_3 is the reaction rate constant. It has been shown^[22] that the reverse of Reaction [5] is not feasible. “n” is an integer having a value of 0, 1, or 2, when occupied sites are considered individually. But the most likely value is 1.

Supposing that Reactions [6] and [7] represent the mechanism of the carbonaceous material-CO₂ reaction, under steady-state conditions, the rate of formation of the occupied site is equal to the rate of their disappearance:

$$d(C_0)/dt = k_1(CO_2)(C_f) - k_2(CO)(C_0) - k_3(C_0) = 0, \quad [8]$$

where (C_0) is the number of occupied sites per gram, and (CO₂) and (CO) are concentrations of CO₂ and CO in the off-gases, respectively.

Assuming that the total number of reaction sites C_t is the summation of free carbon C_f and occupied carbon C_0 as follows:

$$C_t = C_0 + C_f. \quad [9]$$

By substituting Eq. [9] in [8] and rearranging, the following reaction obtained:

$$(C_0) = k_1(CO_2)(C_t)/(k_1(CO_2) + k_2(CO) + k_3). \quad [10]$$

The rate of gasification of carbonaceous materials which are surrounded by a gas can be expressed as follows:

$$dN_C = dn/dt = -k_3(C_0)dW/dt, \quad [11]$$

where dN_C is the rate of carbon transfer from the solid phase to the gas phase and W is the mass of the carbonaceous material. In Eq. [11], after replacing (C_0) with Eq. [10] and rearranging, the following equation is derived:

$$dN_C = -k_3(C_t)/(1 + (CO)/K_1(CO_2))dW. \quad [12]$$

Under steady-state conditions, an integral equation could be derived as follows:

$$\int_0^{N_C} (K_1 + (CO)/(CO_2))dN_C = - \int_{W_0}^{W_1} k_3 K_1(C_t)dW \quad [13]$$

when no CO is injected into the inlet the gas, oxygen and carbon balances at any particular time could be assumed as follows:

$$N_C = N_{CO_2}^0 - N_{CO_2} = (1/2)N_{CO}, dN_C = -dN_{CO_2}, \quad [14]$$

where $N_{CO_2}^0$, N_{CO_2} , and N_{CO} are the initial rate of CO₂, and the rates of CO and CO₂ at any particular time. By substituting Eq. [14] in [13], the following equation is derived:

$$\int_{N_{CO_2}^0}^{N_{CO_2}} (K_1 + 2N_{CO_2}^0/N_{CO_2} - 2)dN_{CO_2} = \int_{W_0}^{W_1} k_3 K_1(C_t)dW. \quad [15]$$

The weight loss could be obtained from the moles of CO (n_{CO}) evolving from the sample:

$$W_t - W_0 = \Delta W = - \sum_{t=0}^{t=l} n_{CO} \times 12. \quad [16]$$

After integration of Eq. [15], the following equation is derived:

$$2(1 + 2/X) \ln(1 + X/2) - 2 = -K_1 + K_1 k_3(C_t)(1 + 2/X)(\Delta W / N_{CO_2}^0), \quad [17]$$

where X represents $X = N_{CO} / N_{CO_2}$.

$2(1 + 2/X) \ln(1 + X/2) - 2$ vs $(1 + 2/X)(\Delta W / N_{CO_2}^0)$ was plotted for the three carbonaceous materials of coke, RDC, and coke-RDC blend. The plot resulted in straight lines as illustrated in Figures 4, 5, and 6. The slope of the straight line and negative intercept with the y axis corresponds to the value of $K_1 k_3(C_t)$ and K_1 , respectively. The values of K_1 and $k_3 C(t)$ calculated from the Figures 4, 5, and 6 for the gasification of coke, RDC, and coke-RDC blend were presented in Table IV. The values of $k_3 C(t)$ obtained from Figures 4, 5, and 6, should be multiplied by $6.023 \times 10^{23} / 22.4 \times 10^3$ to convert them to site/g s.

As shown in Table IV, the equilibrium constant value (K_1) of oxygen exchange reaction of RDC, coke, and coke-RDC samples are equal to 3.1, 1.1, and 1.3, respectively. Equilibrium constant is a function of

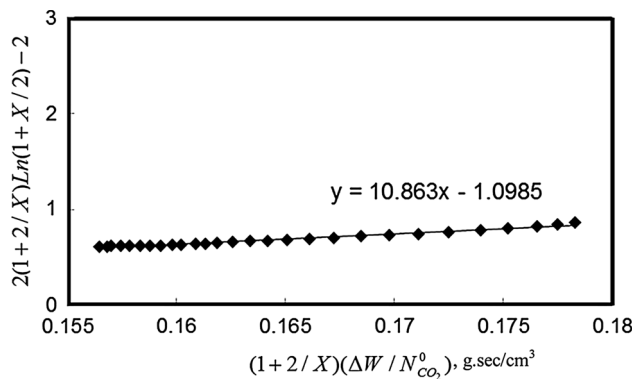


Fig. 4—Reaction of coke with CO_2 -Ar mixture in atmospheric pressure at 1823 K (1550 °C).

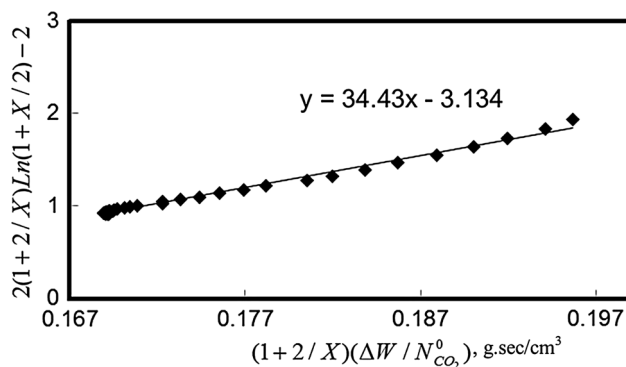


Fig. 5—Reaction of RDC with CO_2 -Ar mixture in atmospheric pressure at 1823 K (1550 °C).

temperature and is independent of the source and its physical properties. The difference in the value of equilibrium derived for RDC, coke, and coke-RDC samples could be attributed to the error involved in the procedure. In a work reported by, Reference 24 the value of K_1 at 1423 K (1150 °C) was measured to be ~1.4 for three types of carbon (*i.e.*, activated carbon, activated graphite, and Ceylon graphite). In the same work, K_1 value for the case of Ceylon graphite increased up to 4.5 when temperature raised to 1673 K (1400 °C). In another work done by, Reference 18 the value of K_1 of pure carbon at [1023 K, 1073 K and 1123 K (750 °C, 800 °C and 850 °C)] was also reported as 0.077, 0.122, and 0.167, respectively.

The value of $k_3 C(t)$ for coke, RDC, and coke-RDC samples are in the range of 9 to $12 \times 6.023 \times 10^{23} / 22.4 \times 10^4$ site/g s. RDC sample has the highest value of carbon transfer rate from the solid phase to the gas phase from occupied sites around 11.6 site/g s ($\times 6.023 \times 10^{23} / 22.4 \times 10^4$). Given that gasification step is the slowest step and the high rate of oxygen exchange of RDC, it can be concluded that RDC has the fastest rate of reaction with CO_2 at 1823 K (1550 °C).

D. Physical Structure and Morphology

The structure of carbonaceous materials is among the numerous factors influencing their reactivity. Raman spectroscopy has been used extensively to characterize the structural features of carbonaceous materials. Figure 7, presents the Raman spectra of the samples after heat treatment, without slag.

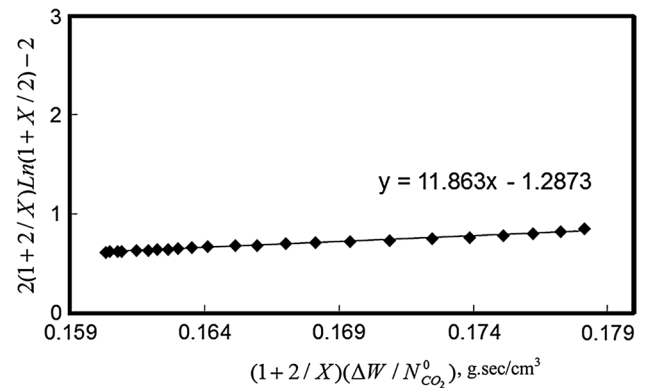


Fig. 6—Reaction of coke-RDC blend with CO_2 -Ar mixture in atmospheric pressure at 1823 K (1550 °C).

Table IV. Equilibrium and Rate Constants of the Reaction of Coke, RDC, and Coke-RDC Blend with CO_2 -Ar Mixture Gas

Carbon Source	K_1	$k_3(C_t)$, site/g s ($\times 6.023 \times 10^{23}$)
Coke	1.1	9.9
RDC	3.1	11.6
Coke-RDC blend	1.3	9.1

In investigating the structure of carbonaceous materials using exciting laser, it is accepted that the D band centered at 1360 cm^{-1} reflects defect and disorder in the graphitic structure of carbon and that the G band at 1585 cm^{-1} represents the graphitic order which is due to E_{2g}^2 fundamental vibration. In well-ordered and organized carbon structures (*i.e.*, graphitized carbons), the G band is more intense than D band.

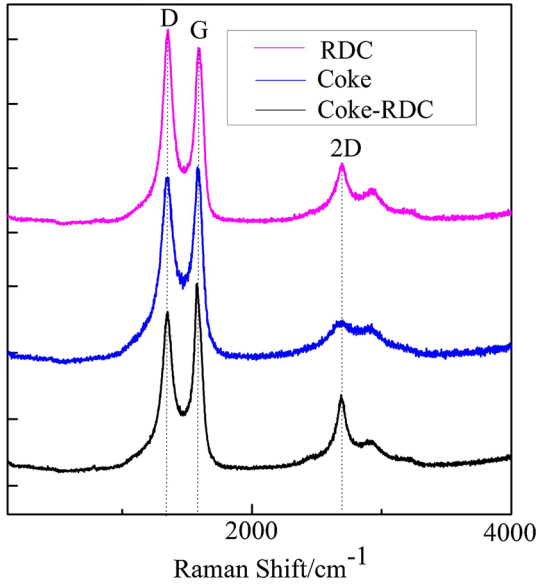


Fig. 7—Raman spectra of coke, RDC, and coke-RDC blend after heat treatment in argon at 1823 K (1550 °C) without slag.

It can be clearly seen from the spectrum of RDC in Figure 7, that the degree of structural order is limited. However, in the case of coke-RDC blend, the spectrum exhibits a stronger peak at 1585 cm^{-1} (G band) compared to 1360 cm^{-1} (D band), implying a highly graphitized structure for coke-RDC blend. The intensity of peak at 1360 cm^{-1} , is stronger than the intensity of the G band which is a convincing sign that RDC sample has less graphitized structure than the coke-RDC blend sample. The changes that occur in the structure of coke and RDC after blending, can be attributed to the aromatization of the aliphatic intermediates resulting from the decomposition of rubber, causing the defects and gaps in the structure of the coke. In fact, the presence of polymeric matters can result in bridging the gaps in the turbostratic structure of carbon and reducing the defects in its structure.

The high equilibrium constant of the oxygen-exchange reaction and the gasification of the RDC sample are attributed to the presence of sp^3 -hybridized carbon atoms in the RDC sample, while in coke-RDC and coke samples, sp^2 -hybridized carbon atoms are present, which were more difficult to break.

In the reactions between the molten slag and carbonaceous materials, the reduction of iron oxide occurs through intermediate CO/CO₂ gases; however, the initial contact between solid carbon and molten slag plays a key role as the CO gas evolved from this reaction will reduce FeO in later stages Reactions [1] and [2]. The high reactivity of RDC in reaction with CO₂ provides evidence that in the interaction between RDC and molten slag, the Boudouard reaction is fast; however, the low rate of iron oxide reduction, shown in

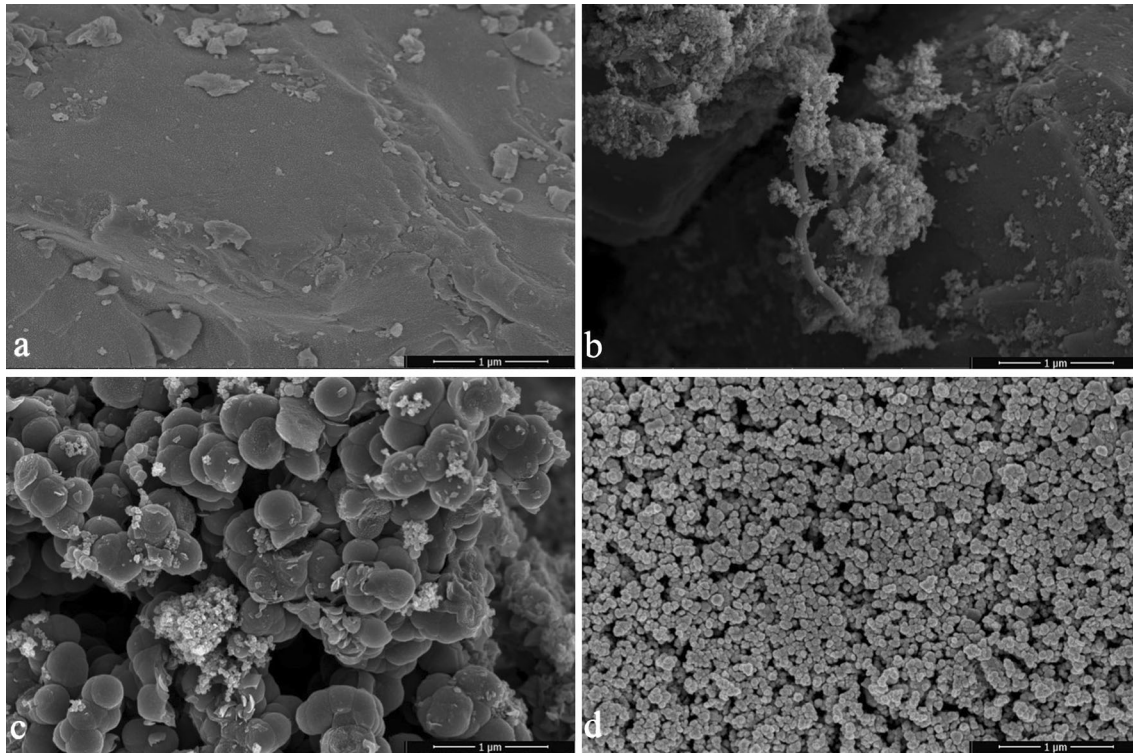


Fig. 8—FE-SEM image of (a) coke; (b, c) coke-RDC blend and (d) RDC after heat treatment in argon at 1823 K (1550 °C) without slag.

Figure 1(b), can be attributed to weak initial contact between the RDC and molten slag. In the coke-RDC sample, due to its well-graphitized structure, confirmed by Raman analysis, the initial, mass transfer between molten slag and coke-RDC sample might be high. During the carbonization, the RDC sample decomposes very quickly resulting in almost pure carbon. However, in coke-RDC sample, some functional groups are believed to present which facilitate better contact between molten slag and coke-RDC sample.

The morphologies of the coke, RDC, and coke-RDC samples prior to addition of slag were also studied using FE-SEM. Figure 8 displays the nano-structural features of the coke, RDC, and coke-RDC blend samples. While in the coke sample (Figure 8(a)) nano-structural feature is not observed, the RDC and coke-RDC samples have morphologies with nano-structural features. In the RDC sample (Figure 8(d)), nano-carbon particles with a diameter of 30 to 40 nm are observed. It should be noted that the particle size of RDC sample is homogeneous. In RDC-coke blend (Figures 8(b) and (c)), several morphologies of carbon can be observed. In RDC-coke sample, carbon particles are observed in the form of nano-particles and nano-tubes as well as light gray bulk areas. SiC particles are also observed, in spherical form with a diameter of 400 to 500 nm, in the coke sample (Figure 8(c)). The high reactivity of the RDC sample in CO₂ can be also attributed to its large surface area.

IV. CONCLUSIONS

The effect of partial substitution of metallurgical coke with waste tyre rubbers (WTR) on the reduction of iron oxide from molten slag was studied. Coke, rubber-derived carbon (RDC), and a coke-RDC blend in particular ratio (the ratio was selected based on previous work on slag foaming) of the same particle size were prepared.

1. In the reduction of FeO from molten slag using coke, RDC, and coke-RDC blend as carbon sources, the coke-RDC blend had the highest rate of reduction, with the highest concentration of gases evolving from the system due to reduction. The RDC sample showed a poor performance in reducing iron oxide from slag.
2. The disordered structure and high defect rate in the aliphatic structure of the RDC resulted in a faster reaction between carbon atoms and CO₂. The kinetics of the reaction of the coke, RDC, and coke-RDC blend samples with CO₂ (5 wt pct)-Ar (96

wt pct) mixture in atmospheric pressure was also studied. RDC samples exhibited the highest rate of gasification step ($11.6 \text{ site/g s } (\times 6.023 \times 10^{23} / 2.24 \times 10^4)$).

3. The high reactivity of the RDC in reaction with CO₂ provided evidence that in the interaction between RDC sample and the molten slag, the Boudouard reaction was fast. The low reaction rate of FeO reduction with RDC could be attributed to weak initial contact between RDC and molten slag.

REFERENCES

1. D.L. Schroeder: *Steel Times*, 2000, vol. 32, pp. 368–72.
2. V. Sahajwalla, L. Hong, and C.N. Saha: *AISTech*, Association for Iron and Steel Technology, Warrendale, PA, USA, AIST, 2005, p. 597.
3. V. Sahajwalla, R. Khanna, M. Rahman, Z. Huang, E. Tanaka, N.C. Saha, D. Knights, and P. O’Kane: *AISTech*, Association for Iron and Steel Technology, Warrendale, PA, USA, 2005, p. 547.
4. M. Rahman, V. Sahajwalla, R. Khanna, N.C. Saha, D. Knights, and P. O’Kane: *AISTech*, Association for Iron and Steel Technology, Warrendale, PA, USA, 2005, p. 491.
5. S. Gupta, V. Sahajwalla, and J. Wood: *Energy Fuel*, 2006, vol. 20, pp. 2557–63.
6. M. Zaharia, V. Sahajwalla, R. Khanna, P. Koshy, and P. O’Kane: *ISIJ Int.*, 2009, vol. 49, pp. 1513–21.
7. M. Zaharia, V. Sahajwalla, B.-C. Kim, R. Khanna, N.C. Saha, P. O’Kane, and J. Dicker: *Energy Fuel*, 2009, vol. 23 (5), pp. 2467–74.
8. V. Sahajwalla, M. Zaharia, S. Kongkarat, R. Khanna, N.C. Saha, and P. O’Kane: *Energy Fuel*, 2010, vol. 24, pp. 379–91.
9. S. Maroufi, I. Mansuri, P. O’Kane, C. Skidmore, Z. Jin, A. Fontana, M. Zaharia, and V. Sahajwalla: *10th International Conference on Molten Slag, Fluxes and Salts, TMS (The Minerals, Metals & Materials Society)*, Seattle, USA, 2016.
10. M. Ozawa, S. Kitagawa, S. Nakayama, and Y. Takesono: *ISIJ*, 1986, vol. 26, pp. 621–28.
11. F.T. Lee and C.H. Lee: *Steel Times Int*, 1995, pp. 20–25.
12. F.-Z. Ji, M. Barati, K. Coley, and A.G. Irons: *VII International Conference on Molten Slags Fluxes and Salts*, The South African Institute of Mining and Metallurgy, 2004, pp. 399–406.
13. M. Rahman: PhD thesis, The University of New South Wales, Sydney, Australia, 2009.
14. S.L. Teasdale and P.C. Hayes: *ISI Int.*, 2005, vol. 45, pp. 634–41.
15. T. Nagasaka, M. Hino, and S. Ban-Ya: *Metall. Mater. Trans. B*, 2001, vol. 31B (5), pp. 945–55.
16. V. Sahajwalla, M. Zaharia, S. Kongkarat, R. Khanna, M. Rahman, N.S. Chaudhury, P. O’Kane, J. Dicker, C. Skidmore, and D. Knights: *Energy Fuels*, 2012, vol. 26, pp. 58–66.
17. R.K. Paramguru, R.K. Galgali, and H.S. Ray: *Metall. Mater. Trans. B.*, 1997, vol. 28B, pp. 805–10.
18. S. Ergun: *J. Phys. Chem.*, 1956, vol. 60, pp. 480–5.
19. S. Ergun: *Ind. Eng. Chem.*, 1955, vol. 47, pp. 2075–80.
20. S. Ergun: *Chem. Eng. Progr.*, 1952, vol. 48, pp. 227–36.
21. S. Ergun: *Anal. Chem.*, 1951, vol. 23, pp. 151–56.
22. A.E. Reif: *J. Phys. Chem.*, 1952, vol. 56, pp. 785–88.
23. H Freund: *Fuel*, 1986, vol. 65, pp. 63–66.
24. M Mentser and S Ergun: *Carbon*, 1967, vol. 5, pp. 331–37.